

VORTEX-INDUCED VIBRATIONS OF LINE-LIKE STRUCTURES

Svend Ole Hansen (member), Svend Ole Hansen ApS, Denmark
Presented at CICIND's 50th Meeting, Oxford, September 1998

1. Introduction

Although a great deal of effort has been made during recent decades to improve the analytical models used for predicting vibrations due to vortex shedding, the analytical models available are still rather crude. The cross-wind forcing mechanisms have proved to be so complex that there is no general analytical method available to calculate cross-wind structural response. The main physical parameters involved in the forcing mechanisms have been clarified, but the basic data used in full-scale predictions have not reached general agreement among researchers.

Some of the most important pioneering research contributions during approximately the last 20–30 years have come from the University of Western Ontario (UWO) in Canada and the Technical University of Aachen (RWTH) in Germany. These two research groups have directed their efforts to identifying different aspects of vortex-induced vibrations. However, the methods they use to take aeroelastic effects, i.e. motion-induced wind loads, into account differ considerably.

The design procedure proposed here is based on the UWO-mathematical spectral model originally suggested by Vickery and Clark (1972) and further refined by Vickery and Basu (1983). However, their spectral model is here extended to include the influence of turbulence in the vibration amplitude predictions. The inclusion of turbulence changes the predictions considerably towards the behaviour observed for many full-scale steel chimneys.

Two primary design aspects will be focused on in the design procedure proposed:

1. Rare, extreme events occurring say once in 10–50 years. These events are important in connection with damage potential or alarming bystanders and their contribution to fatigue should also be analysed.
2. Frequent events occurring many times during the expected lifetime. These events will often give the major contributions to the fatigue damage calculated.

It is essential that both aspects mentioned above are included in design models for vortex shedding. The present model used in Eurocode 1 (1995) provides estimates, which are larger than the frequent events and lower than the rare events, see Dyrbye and Hansen (1996). The present Canadian Code (1990) and the present CICIND (1989) model code focus primarily on the rare events, i.e. overestimate the frequent events considerably.

The design procedure proposed here takes rare as well as frequent events into account by including the influence of turbulence in the vibration amplitude predicted. This ensures that rare events are not underestimated as in Eurocode 1 (1995) and that frequent events are not overestimated as in other codes, e.g. the CICIND (1989) model code.

It is hoped that this more realistic design approach, including the influence of turbulence, could be used in the efforts to direct the different research groups toward a common understanding regarding vortex-induced vibrations of line-like structures.

All chimneys considered in the paper are isolated, i.e. not part of a group. Group effects are, therefore, not considered. Only chimneys with circular cross sections are part of the study.

2. Vortex-induced vibrations based on the spectral model

Originally, Vickery and Clark (1972) proposed the spectral model used to predict vortex-induced vibrations of line-like structures. During the last approx. 25 years the formulation and aerodynamic parameters used in the model have been analysed in several papers and text books, see e.g. Vickery and Basu (1983), Vickery (1998) and Dyrbye and Hansen (1996).

The large vortex-induced vibrations may occur when the mean wind velocity is equal to the resonance wind velocity, i.e.

$$v_m = v_r = \frac{n_e d_{ref}}{St} \quad (1)$$

in which n_e is the natural frequency, d_{ref} is the reference width and St is Strouhal number. Of course, the vortex-induced vibrations calculated do not depend on the choice of reference quantities, e.g. the reference width. For chimneys the reference quantities chosen often refer to the point, at which the structural vibrations are largest, i.e. at the chimney top for the fundamental mode of vibration.

Assuming that the reference velocity pressure is given by:

$$q_{ref} = \frac{1}{2} \rho d_{ref}^2 n_e^2 / St^2,$$

in which ρ is the air density, the standard deviation σ_y of the structural deflection is given by, see Dyrbye and Hansen (1996) equation (7.4.8)

$$\frac{\sigma_y(z)}{d_{ref}} = \frac{C_0 C_1}{St^2} \frac{\rho d_{ref}^2 m_e}{\sqrt{\zeta_s - \zeta_a}} \sqrt{\frac{d_{ref}}{h}} \frac{\xi(z)}{\xi_{ref}} \quad (2)$$

in which ζ_s and ζ_a are the structural and aerodynamic damping ratios, respectively. The constants C_0 and C_1 , and the effective mass m_e per unit of length are given by:

$$C_0 = \frac{4\sqrt{\pi}}{8\sqrt{2\pi^2}} \frac{\tilde{C}_{L,ref} \sqrt{\lambda}}{\sqrt{B_{ref}}} \quad (3)$$

$$C_1 = \frac{\sqrt{\frac{1}{h} \int_0^h g^2(z, n_e) dz}}{\frac{1}{h} \int_0^h \frac{m(z) \xi^2(z)}{m_e \xi_{ref}^2} dz} \quad (4)$$

$$m_e = \frac{\int_0^h m(z) \xi^2(z) dz}{\int_0^h \xi^2(z) dz} \quad (5)$$

ξ = mode shape

in which the function g introduced in equation (4) is equal to, see Dyrbye and Hansen (1996), equation (7.4.4)

$$g(z, n) = \frac{q(z) d(z) \tilde{C}_L(z) \xi(z)}{(q d \tilde{C}_L)_{ref}} \sqrt{\frac{B_{ref}}{B(z)}} \sqrt{\frac{n}{n_s(z)}} \exp \left[-\frac{1}{2} \left(\frac{1 - n/n_s(z)}{B(z)} \right)^2 \right] \quad (6)$$

where the vortex-shedding frequency $n_s(z) = St \cdot v_m(z) / d(z)$.

The constant C_0 in equation (3) depends on the lift coefficient \tilde{C}_L , the load correlation length λ and the spectral bandwidth B , all parameters describing the vortex-induced wind load on non-vibrating structures. \tilde{C}_L and B , and thereby C_0 , are all functions of turbulence intensity and Reynolds number, see e.g. Vickery (1998).

The constant C_1 in equation (4) depends primarily on the mode shape and to some extent also on the velocity profile and diameter variation with height. Assuming a uniform mode shape and velocity profile, height independent of width d , lift coefficient \tilde{C}_L and spectral bandwidth B , the function $g(z, n_e)$ becomes equal to 1 when the vortex-shedding frequency $n_s(z)$ is equal to the natural frequency n_e for all heights z .

The motion-induced wind loads in the spectral model are taken into account by aerodynamic damping of the form $a\dot{y} - b\dot{y}^3$, where the first, linear, term introduces negative aerodynamic damping and the last, non-linear, term gives positive damping ensuring that the response is self-limiting. For small amplitudes of up to approx. 5% of the structural width, the aerodynamic damping is described sufficiently accurate by the first, linear term.

The aerodynamic damping ratio ζ_a is given by, see Vickery and Basu (1983):

$$\zeta_a = \frac{\rho d_{ref}^2}{m_e} K_{a,ref} \left(C_2 - C_3 \left(\frac{\sigma_{y,ref}}{d_L d_{ref}} \right)^2 \right) \quad (7)$$

in which the constants C_2 and C_3 are expressed as:

$$C_2 = \frac{\int_0^h \frac{K_a(z)}{K_{a,ref}} \frac{d^2(z)}{d_{ref}^2} \xi^2(z) dz}{\int_0^h \xi^2(z) dz} \quad (8)$$

$$C_3 = \frac{\int_0^h \frac{K_a(z)}{K_{a,ref}} \frac{\xi^4(z)}{\xi_{ref}^4} dz}{\int_0^h \frac{\xi^2(z)}{\xi_{ref}^2} dz} \quad (9)$$

Neglecting end effects it is often a good approximation to assume that $K_a(z)$ is independent of height z . For structures with constant width d , C_2 then becomes equal to 1 and the constant C_3 only depends on the mode shape. C_3 becomes equal to 1 and 5/9 for uniform and parabolic mode shapes, respectively. Parabolic mode shapes may, therefore, have larger limiting amplitudes than uniform mode shapes. This is not surprising since the stabilising non-linear damping force acts along a shorter structural length when the mode shape becomes more complex.

Equations (2) and (7) in combination indicate that the Scruton number S_c , defined as:

$$S_c = \frac{2\delta_s m_e}{\rho d_{ref}^2} \quad (10)$$

becomes important for the vortex-induced vibrations. The logarithmic decrement δ_s describing the structural damping is equal to $\delta_s = 2\pi\zeta_s$, where ζ_s is the structural damping ratio.

The discussion below focuses on the motion-induced wind loads and their dependence on end effects, Reynolds number and air turbulence. Especially large scales of the air turbulence are found to be most important for the understanding of observed full-scale behaviours of steel chimneys described in Section 5 and this is a crucial input for a realistic code design procedure, see Section 4.

3. Motion-induced wind loads

The aerodynamic damping parameter K_a governs the motion-induced wind loads on the structure. It depends on end effects, Reynolds number and air turbulence as analysed below in Sections 3.1-3.3.

Surface roughness of a chimney with circular cross section does probably also influence the aerodynamic damping parameter K_a . However, available data are sparse and the fact that surface roughness of steel chimneys typically vary within a relatively narrow band, makes this parameter less important.

3.1 End effects

The end effects have been recognised in many codes specifying minimum slenderness ratios h/d for which vortex-induced vibrations should be taken into account. Vickery (1998) quantifies the end effects for a cantilevered square cylinder by measurements of motion-induced wind loads at different distances from the end. These measurements show that the motion-induced wind load is zero at the cylinder top and that the maximum value occur approx. 3 widths from the top. The actual location of maximum motion-induced wind loads depends on the mode shape in combination with the end effects.

3.2 Reynolds number

It is well known that the Reynolds number is a crucial parameter for wind loads on circular cylinders. The description below refers to stationary cylinders.

For subcritical Reynolds numbers between approx. 300 and approx. 10^5 , the boundary-layer flow at the cylinder surface is laminar, and the points of separation are about 80° from the point of stagnation. Vortices are shed from alternate sides of the stationary cylinder within a relatively narrow frequency band.

For supercritical Reynolds number between approx. 10^5 and approx. 10^6 , points of separation are on the leeward side of a stationary cylinder, and the wake has become much narrower. The cross-wind load on a stationary cylinder is aperiodic and random.

For transcritical Reynolds numbers above approx. 10^6 , the boundary-layer flow at the cylinder surface is turbulent, and the points of separation are about 115° from the point of stagnation. The wake is narrower than in the subcritical range but wider than in the supercritical range. Vortices are shed from alternate sides of the stationary cylinder within a relatively narrow frequency band, thus resembling the subcritical range.

The description above refers to stationary cylinders. However, the relative tendency for vortex-induced vibrations in the different Reynolds number regimes are expected to follow the flow characteristics observed for stationary cylinders.

3.3 Air turbulence

The effect of turbulence on vortex-induced vibrations has been considered experimentally by Vickery (1998), and Krenk & Nielsen (1998) include turbulence in their theoretical lift-oscillator model. The description below extracts the basic influence of air turbulence and proposes a simplified model used to take turbulence into account in practical designs.

Amplitude build-up in low turbulence flow

Figure 1a-c shows the increase in amplitude for a fixed cylinder suddenly released in a wind tunnel with low turbulence flow. The natural frequency of the cylinder vibrations is 1.81 Hz. The upper figure refers to a wind velocity v_m approx. 4% lower than the resonance wind velocity v_r , i.e. $v_m \approx 0.96v_r$, the middle figure to $v_m \approx v_r$ and the lower figure to $v_m \approx 1.05v_r$. The figure shows a slow increase in amplitude where maximum amplitudes are reached after approx. 1000 natural vibration periods. Furthermore, the maximum amplitude reached depends strongly on the ratio between the actual wind velocity and the resonance wind velocity.

Large-scale turbulence in the atmosphere may be interpreted as a slowly varying mean wind velocity. Looking at the results shown in Figure 1a-c, it is not surprising that large scale turbulence will have a pronounced effect on vortex-induced vibrations. When the mean wind velocity for a short period of time is equal to the resonance wind velocity, the amplitudes will grow slowly, but as soon as the mean wind velocity has changed away from the resonance wind velocity,

large amplitudes will not grow up. The actual amplitudes will be of stochastic nature, i.e. increase when the wind velocity is close to the resonance wind velocity and reduce when this is not the case.

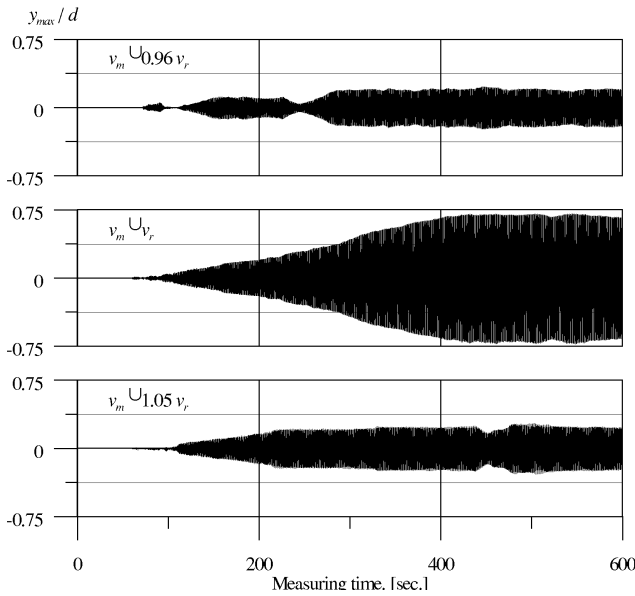


Figure 1a-c.
Built-up of amplitudes after the cylinder has been released in low turbulence flow.

The observations described above refer to structures not having extremely low Scruton numbers. At these low Scruton numbers large vibrations may develop even in turbulent flow, see Figure 5a-d.

The influence of large scale turbulence may be estimated approximately by integrating the aerodynamic damping parameter measured for different mean wind velocities and weighed with a Gaussian distribution describing the variation of the longitudinal turbulent component. A more accurate approach will be to analyse the differential equation describing the variations of the lift coefficient in time. Measurements of aerodynamic damping terms in turbulent flow may also be used.

The aerodynamic damping parameter K_a depends on turbulence intensity and not on the absolute variations of the wind velocity, e.g. expressed by the standard deviation of turbulence.

Vortex-induced vibrations in turbulent flow

The influence of turbulence on vortex-induced vibrations has been investigated in a test with a circular cylinder carried out in our boundary layer wind tunnel in cooperation with the Danish Technical University. Different combinations of low- and high frequency turbulence were investigated, in order to determine the influence of turbulent length scale.

4 different turbulence conditions were tested. Smooth flow is the basic set-up in the tunnel without any turbulence generators. The turbulence intensity is approximately 2–3% and governed by very high frequency turbulence. 3 spires located at the inlet generate additional high frequency turbulence with small scales. The turbulence intensity is approximately 18%. Changing the rotation speed of the ventilator generates low frequency turbulence at frequencies lower than 1–2Hz. The turbulence intensity was approximately 10% at the high level and 7% at the low level. Broad band turbulence is a combination of the low and high frequency turbulence mentioned above. The turbulence intensity was 21%.

The circular cylinder was mounted horizontal in the tunnel. The outer diameter is 20cm, and by using end plates the flow around the cylinder is approximately 2-dimensional. The natural frequency of the spring-supported cylinder is 1.81Hz. The acceleration of the cylinder was measured at the two end-points. The amplitude of the cylinder as a function of the wind speed and structural damping is

shown on the figures on the following pages. Figure 2 shows the standard of the acceleration as a function of Scruton number defined in equation (10). Figure 3 shows the response (standard deviation) for large Scruton numbers.

The critical Scruton number at which the jump from small to large vibrations occur depend strongly on the low frequency turbulence with large scales, but not on the high frequency turbulence with small scales. The critical Scruton number in the present test in low turbulent flow is smaller than other tests indicate. This may be due to end effects in the wind tunnel. The present test results should, therefore, not be used to estimate absolute values of critical Scruton numbers, but to provide data showing the relative influence of turbulence.

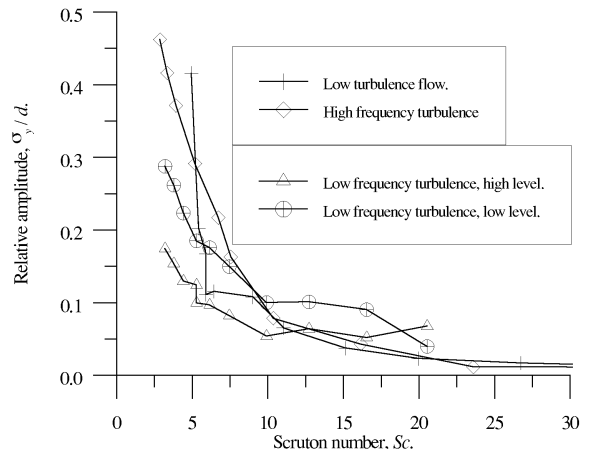


Figure 2.
Relative amplitude as function of Scruton number and turbulence.

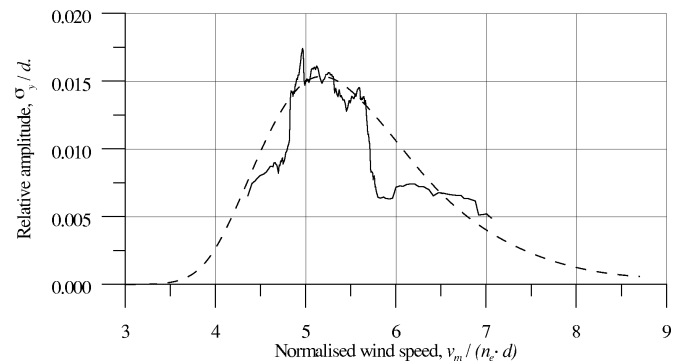


Figure 3.
Relative amplitude for large Scruton numbers as function of the normalised wind speed. The dotted line is theoretical predictions based on equation (17).

4. Code design proposal

The revised Danish wind code expected to be published late 1998 includes the design model for vortex-induced vibrations described below.

Inserting equation (7) in equation (2), and assuming $C_1=1$ and $C_2=1$, the standard deviation of the structural deflection at the reference point where the structural vibrations are largest is given by:

$$\frac{\sigma_y}{d} = \frac{1}{St^2} \frac{C_a}{\sqrt{\zeta_s - K_a \frac{\rho d^2}{m_e} \left(1 - \left(\frac{\sigma_y}{a_L d}\right)^2\right)}} \frac{\rho d^2}{m_e} \sqrt{\frac{d}{h}} \quad (11)$$

in which $C_a = C_0 C_1$ and ζ_s is the structural damping ratio.

The standard deviation of the structural deflection may be determined by solving equation (10). The solution is given by:

$$\left(\frac{\sigma_y}{d}\right)^2 = c_1 + \sqrt{c_1^2 + c_2} \quad (12)$$

where the constants c_1 and c_2 are equal to:

$$c_1 = \frac{a_L^2}{2} \left(1 - \frac{\zeta_s}{K_a} \frac{m_e}{\rho d^2}\right) \quad (13)$$

$$c_2 = \frac{a_L^2}{K_a} \frac{\rho d^2}{m_e} \frac{C_a^2}{St^4} \frac{d}{h} \quad (14)$$

In the present simplified and approximate approach, the aerodynamic damping parameter K_a is estimated for smooth flow cases as a function of Reynolds number. A function of longitudinal turbulence intensity, I_v , gives the reduction in turbulent flow, i.e.:

$$K_a(Re, I_v) = K_{a,max}(Re) \cdot K_v(I_v) \quad (15)$$

The aerodynamic damping parameter, $K_{a,max}$, for smooth flow is given in Table 1 and shown in Figure 4. The function K_v may approximately be determined by $K_v = 1 - 3I_v$ for $0 \leq I_v \leq 0.25$ and $K_v(I_v) = 0.25$ for $I_v > 0.25$. This simplified model takes turbulence into account in a rather crude way and it gives only rough indications. Further studies are needed to clarify the influence of turbulence more accurately.

The maximum amplitude γ_{max} is calculated by multiplying the standard deviation σ_y given by equation (11) with a peak factor k_p , i.e. $\gamma_{max} = k_p \sigma_y$. For small amplitudes below approx. 1–2% of the diameter, the peak-factor is approx. 3.5-4 depending on the natural frequency of the structure. For large amplitudes, the peak-factor is equal to $\sqrt{2}$ and for intermediate amplitudes, the peak-factor increases gradually with decreasing amplitude. The following simplified expression may be used to determine the peak-factor:

$$k_p = \sqrt{2} (1 + 1.2 \tan^{-1} (0.75 (Sc/(4\pi K_a)^4))) \quad (16)$$

Table 1. Aerodynamic parameters in smooth flow. For Reynolds numbers between 10^5 and $5 \cdot 10^5$, and between $5 \cdot 10^5$ and 10^6 , the aerodynamic parameters are determined by linear interpolation using $\ln(Re)$ as argument.

Aerodynamic parameter	$Re \leq 10^5$	$Re = 5 \cdot 10^5$	$Re \geq 10^6$
$C_{a,max}$	0.02	0.005	0.01
$K_{a,max}$	2	0.5	1
a_L	0.4	0.4	0.4

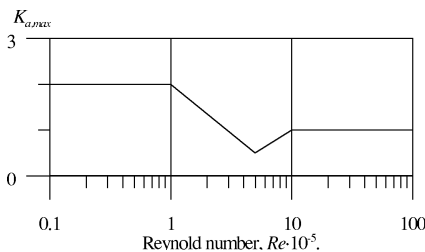


Figure 4.

The aerodynamic damping parameter $K_{a,max}$ for smooth flow as function of Reynolds number.

The variation of $K_{a,max}$ with Reynolds number follows the description in Section 3.2 for a stationary cylinder and it is in agreement with test results and full-scale observations.

Inserting $K_{a,max}$ in equation (11) gives the vibrations amplitudes illustrated in Figure 5a for smooth flow at different Reynolds numbers. Figure 5c–d show the vortex-induced vibrations as function of turbulence intensity for the Reynolds numbers considered in Figure 5a.

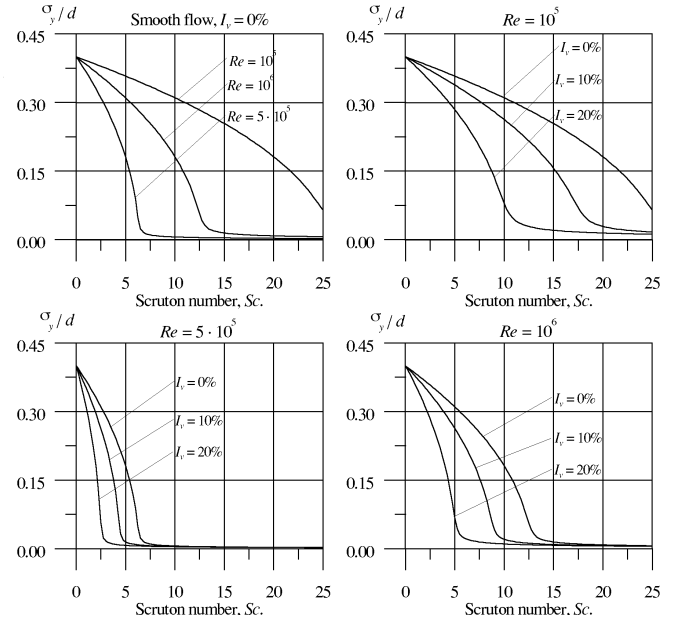


Figure 5a–d.

Vortex-induced vibrations as function of turbulence intensity and Reynolds number. It is assumed that $m_e/\rho d^2 = 50$ and $h/d = 30$, which influence the low amplitude part of the curves shown.

The estimates of $K_{a,max}$ specified in Table 1 are primarily based on measurements on model-scale and full-scale chimneys. However, the scatter of these measurements is considerable, indicating that the $K_{a,max}$ estimates are encumbered with some uncertainty. One of the criteria for the $K_{a,max}$ calibrations carried out has been that the large vibrations observed on the full-scale chimneys considered in Table 2 could be predicted using the code proposal. These calibrations have been based on structural damping values specified in the Eurocode 1 (1995) whenever the structural damping is unknown.

The value of $K_{a,max}$ is crucial in order to estimate reliable results in the rare events of meteorological conditions with smooth air flow and at mean wind velocity equal to the resonance wind velocity. When large vortex-induced vibrations are not allowed in the design due to serviceability, and the resonance wind velocity has a magnitude making smooth flow possible, it is not important how the aerodynamic damping parameter K_a depends on turbulence intensity and on the ratio v_m/v_r between mean wind velocity and resonance wind velocity. This conclusion follows from the fact that K_a is only important for the critical Scruton number, where the vortex-induced response is changed from large harmonic amplitudes to small stochastic amplitudes, see Figure 5. If large vibrations are avoided it is only the parameters governing the small stochastic amplitude motions which become important. If the resonance wind velocity has a magnitude where some turbulence is inevitable, the damping parameter as function of turbulence becomes important.

Fatigue calculations

Fatigue calculations could be carried out combining the probability of different turbulence intensities for wind velocities close to the critical wind velocity with stress calculations using the design procedure proposed. The occurrence of different atmospheric stability conditions is, therefore, important.

The constants C_a and K_a depend on the wind velocity ratio v_m/v_r , where v_m is the mean wind velocity and v_r is the resonance wind velocity. They are approximately given by:

$$C_a = C_{a,\max} \left(\frac{v_m}{v_r} \right)^{3/2} \exp \left[-\frac{1}{2} \left(\frac{1-v_r/v_m}{B} \right)^2 \right] \quad (17)$$

$$K_a = K_{a,\max} (\text{Re}) \cdot K_v(I_v) f(v_m/v_r) \quad (18)$$

The function f has its maximum value of 1 for $v_m = v_r$, and it may, as a rough approximation, be assumed to decrease linearly to the value of 0 for $v_m = 2v_r$. The function f is roughly equal to 0 for $v_m < v_r$, and for $v_m > 2v_r$.

The occurrence of mean wind velocities up to approx. 15–20m/s could be based on information included in the European Wind Atlas. Originally, this information was intended to be used in connection with predictions of wind energy production from wind turbines, but the European Wind Atlas will in most cases also provide accurate wind data input for use in calculating fatigue damage due to vortex shedding.

The occurrence of different turbulence intensities as a function of mean wind velocity has not been investigated thoroughly in the past. In connection with the Danish wind code revision, the results from two wind measuring stations were used to establish distributions of turbulence intensities. Both stations are characterised by wind over land with roughness lengths z_0 of between 0.01m and 0.05m. For the two stations analysed, the occurrence of different turbulence intensities $I_v(z)$ at height z may approximately be given by a Gaussian distribution with:

- mean value corresponding to neutral atmospheric conditions, i.e. $I_v(z) = 1/\ln(z/z_0)$
- standard deviation, which gradually decreases from approx. 0.06 at mean wind velocities below approx. 5m/s to approx. 0.03 for mean wind velocities of approx. 10m/s.

The probability connected with negative arguments may be assumed to correspond to zero turbulence intensity. The probabilities of turbulence intensities based on the Danish measurements will probably overestimate low turbulence situations in most parts of Europe thereby leading to overestimated fatigue damage of the structure.

Comparisons with the CICIND (1989) model code

The design procedure proposed in this note is based on the mathematical model originally suggested by Vickery and Clark, i.e. the same basic model as used in the CICIND (1989) model code. However, the present design procedure and the CICIND specifications differ considerably on several aspects:

1. The influence of turbulence has been included in the present design procedure in order to take observations on full-scale chimneys duly into account.
2. In the present design procedure, the aerodynamic damping parameter K_a specifying the motion-induced forces depends on the Reynolds number in the same way as the lift coefficient. This dependence is in agreement with quasi-static approaches, but it is not in accordance with the aerodynamic damping parameter specified in the CICIND (1989) model code.
3. The Strouhal number, the mass ratio and the slenderness ratio are used to calculate the structural vibrations in the design model proposed. These parameters are not included specifically in the CICIND model code.

5. Full-scale observations versus code predictions

Full-scale observations of steel chimneys have been reported extensively, see e.g. Pritchard (1984), Daly (1986) and Dyrbye & Hansen (1996). Some of these observations are described in Section

5.1 and in Section 5.2, the observations are compared with code predictions based on Eurocode 1 (1995), CICIND (1989) model code and the code proposal included in Section 4.

5.1 Full-scale observations

The full-scale observations considered in the paper are tabulated in Table 2–4 on the last pages of the paper. Some characteristic features are discussed below in connection with the Danish chimneys considered.

Full-scale measurements on four Danish steel chimneys were carried out in the late 1970s, see Frandsen (1979). They were part of a research project that primarily aimed to improve the prediction accuracy regarding the vortex shedding response of steel chimneys. None of the chimneys used in the project had experienced unacceptable vibrations during service. Natural frequencies and structural damping were determined by ambient vibration tests and wind-induced vibration amplitudes were measured.

According to the measurements carried out in the late 1970s none of the four chimneys experienced large vibrations due to vortex shedding. However, approx. 15 years later on December 22, 1995 one of these four chimneys experienced unacceptably large vibrations. The chimney in question is located in Thyborøn and the large vibrations caused a 1 m long crack in the shell near the gas pipe inlet. A tuned mass damper has now been installed at the top of the chimney.

During the winter in 1995/96 four Danish chimneys have all experienced unacceptable large vibrations, the Thyborøn chimney being one of the four. All four chimneys were constructed during the period from 1972 to 1980, and no serious vibrations had been reported until the large vibrations occurred during the winter in 1995/96, i.e. approx. 20 years after construction.

The large amplitudes generate considerably noise, which often is what draws people's attention to the vibrations in the first place. The large vibrations cause great concern to neighbours and employees of the plant where the chimney is located.

The chimney in Herning was first observed to vibrate alarmingly by neighbours who heard the noise when returning home after Christmas Eve dinner. All people in the neighbourhood observed the vibrations of the chimney in Odense. These vibrations were reported in one of the major Danish newspapers as reaching amplitudes of approx. 3m. The article focused on the major risk of a 75m tall chimney collapsing in the middle of Odense city centre.

The large vibrations of all 4 chimneys were observed during periods of cold weather with temperatures of approx. -10°C to -5°C . These vibrations occurred primarily in the morning and / or in the evening, indicating that the air flow may be characterised by extremely low turbulence levels due to stable stratification of the atmosphere.

The observations made during the winter 1995/96 were not unique. Approx. 10 years earlier, several steel chimneys were observed to vibrate violently at different locations in Denmark.

It should be emphasised that the large vibrations described above are not caused by group effects or corrosion problems. Furthermore, the large vibrations are not judged to originate from structural or foundation changes due to the cold weather. Rare events with large vibrations have also occurred during weather conditions with temperatures well above 0°C . However, the probability of low turbulence situations in cold weather is larger than in normal weather situations.

5.2 Code predictions

In Figure 6, the full-scale vibrations of 7 steel chimneys, 1 distillation column and 1 antenna mast are compared with the theoretical predictions based on Eurocode 1 (1995). All have Scruton numbers below approx. 10, making them susceptible to vortex-induced vibrations. The main structural data are given in Table 2.

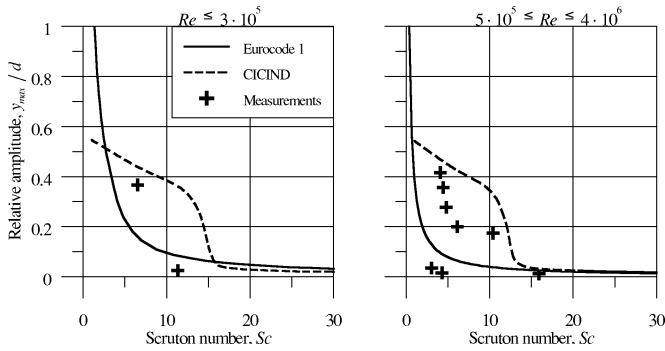


Figure 6.

Comparisons between relative amplitudes measured full-scale and relative amplitudes predicted using CICIND model code and Eurocode 1 (1995). From Dyrbye and Hansen (1996).

According to the results shown, under special conditions, e.g. certain meteorological situations with cold and smooth air flow over a relatively long period of time, say of approximately 1 hour, some slender steel structures may experience larger vibrations than predicted by Eurocode 1 (1995).

In conclusion, Eurocode 1 (1995) sometimes overestimates and sometimes underestimates the response caused by vortex shedding. There seems to be a need for adjustments of the calculation procedure specified and in the basic parameters used to estimate the response. The meteorological situations that lead to larger vibration amplitudes than predicted using Eurocode 1 should be clarified.

The large air density in cold weather with a barometric pressure above normal standard should be taken into account calculating the Scruton number.

The vibration amplitude and structural damping of the 80m steel distillation column, see Table 2, are based on actual measurements that are expected to be reliable. The structural damping of the antenna mast, see Table 2, has also been measured carefully. The Polish and some of the Danish vibration amplitudes, see Table 2, are based on observations, which might overestimate the actual vibration amplitudes. However, the uncertainties related to observations are not expected to be able to explain the large discrepancies, where responses observed are of the order of 5 times larger than the vibration amplitudes calculated using Eurocode 1 (1995).

Pritchard (1984) has reported several observations of vibrating full-scale steel chimneys, see Table 4, which comprises the chimneys with no group effects.

Figure 7 below shows the ratio between observed amplitudes and predicted ones using the design procedure proposed. This response ratio is illustrated as function of Reynolds number for all structures in Table 2–4, where smooth flow has been assumed, i.e. for resonance wind velocities below a somewhat arbitrary limit velocity here chosen to 11m/s.

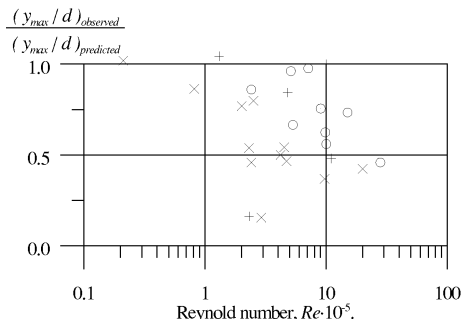


Figure 7.

Response ratio as function of Reynolds number for smooth flow. o: Table 2, +: Table 3 and ×: Table 4.

Figure 7 shows that the code procedure proposed is able to predict all large vibrations observed on the structures tabulated in Table 2–4. This is promising remembering that only the structures in Table 2 have been used in the calibration of the design procedure.

6. Conclusion

Full-scale observations on many steel chimneys suggest that large and violent vortex-induced vibrations sometimes occur as rare, extreme events and that typical and frequent vortex-induced vibrations occur with much smaller amplitudes.

Eurocode 1 (1995) estimates vibration amplitudes, which are larger than the frequent events and lower than the rare events. The present CICIND (1989) model code focuses primarily on the rare events, i.e. overestimates the frequent events considerably.

The paper presents a new code design proposal able to predict vortex-induced vibrations of line-like structures. The procedure is based on the spectral model originally suggested by Vickery & Clark (1972). The model is here extended to cover smooth as well as turbulent flow. The inclusion of turbulence in the model facilitates predictions similar to the full-scale behaviour observed on many steel chimneys. The rare, extreme events occur in smooth air flow and turbulent flow gives the frequent vortex-induced small amplitude vibrations.

The new code design proposal is able to predict all large vibrations observed on the structures considered, see Table 2–4, and the predictions are always larger than or approximately equal to the observed vibration amplitudes.

The accuracy of the new design procedure proposed could be improved further by new research studies. One aspect that should be focused on is the motion-induced wind load described by the aerodynamic parameter K_a and its dependence on turbulence, Reynolds number and end effects. Furthermore, the distribution of different turbulence intensities as a function of mean wind velocity should be estimated at typical locations throughout Europe in order to establish realistic meteorological assumptions used for fatigue calculations of structures susceptible to vortex shedding. The turbulence distributions presented in the paper originate from Danish wind measurements, and will for most sites in Europe probably overestimate the probability of low turbulence situations and thereby lead to overestimated fatigue damage estimates.

7. Acknowledgements

The many valuable and constructive comments from Mr. B.N. Pritchard (Chairman, CICIND steel chimney committee) and Mr. H. Van Koten (Flow Engineering B.V.) are highly acknowledged.

8. References

- Vickery, B.J. (1998): "Wind loads & design criteria for chimneys". CICIND report, Vol. 14, No. 2, 1998.
- Berger, G.W. (1999): "Measured damping decrements of steel chimneys and their estimation in view of the type of the chimneys". CICIND report, Vol. 15, No. 1, 1999.
- Dyrbye, C. and Hansen, S.O. (1996): "Wind Loads on Structures". John Wiley & Sons, 1996.
- Eurocode 1 (1995): "Basis of design and actions on structures. Part 2-4 : Actions on structures — Wind actions". European Prestandard ENV 1991-2-4.
- Daly, A.F. (1986): "Evaluation of methods of predicting the across-wind response of chimneys". CICIND report, Vol. 2, 1986.
- Pritchard, B.N. (1984): "Steel chimney oscillations: a comparative study of their reported performance versus predictions using existing techniques". Eng. Struct., Vol. 6, October 1984.

7. Vickery, B.J. and Basu, R.I. (1983): “*Across-wind vibrations of structures of circular cross-section. Part 1. Development of a mathematical model for two-dimensional conditions*”. Journal of Wind Engineering and Industrial Aerodynamics, Vol. 12, pp. 49–73, 1983.

8. Van Koten, H. (1979): “*Experiences with cross wind vibrations of towers and stacks*”. Symposium on Practical Experiences with Flow-induced Vibrations, Karlsruhe, Germany, 1979.

9. Ruscheweyh, H. and Hirsch, G. (1975): “*Full scale measurements of the dynamic response of tower shaped structures*”. Fourth International Conference on Wind Effects on Buildings and Structures, London 1975.

10. Johns, D.J.; Britten, J. and Stoppard, G. (1972): “*On increasing the structural damping of a steel chimney*”. Earthq. Eng. Struct. Dyn., Vol. 1, 1972, pp. 93–100.

11. Zorilla, E.P. (1972): “*Determination of aerodynamic behaviour of cantilevered stacks and towers of circular cross section*”. ASME Publ. 71-Pet-36, June 1972.

12. Vickery, B.J. and Clark, A.W. (1972): “*Lift or across-wind response of tapered stacks*”. Journal of Structural Division, ASCE, Vol. 98, pp. 1–20.

13. Nakagawa, K. et al. (1963): “*An experimental study of aerodynamic devices for reducing wind-induced oscillatory tendencies in stacks*”. International Conference on Wind Effects on Buildings and Structures, NPL, June 1963.

14. Scruton, C. (1955): “*Wind excited oscillations of tall stacks*”. The Engineer, Vol. 99, London 1955.

Table 2. Chimneys from Denmark, Belgium and Poland. Distillation column from Canada and antenna mast from Norway.

Identification — location:			Aarhus Denmark	Thyborøn Denmark	Odense Denmark	Herning Denmark	Knokke Belgium	Dist. col. Canada	Pol. A Poland	Pol. B Poland	Vealøs Norway
Reference:			Personal Commun.	Dyrb.&Han. 1996	Dyrb.&Han. 1996	Dyrb.&Han. 1996	Personal Commun.	Basu 1983	Ciesielski 1992	Ciesielski 1992	Personal Commun.
Measured / estimated refer to damping:			Est.	Meas.	Est.	Est.	Est.	Meas.	Meas.	Meas.	Meas.
height	h	[m]	56	64	75	56	50	80	26	30	12.5
diameter	d	[m]	2.2	2.8	2.4	1.8	1.6	3.96	1.25	0.816	1.61
slenderness ratio	h/d	[-]	25	23	31	31	31	20	21	37	8
natural frequency	n_e	[Hz]	0.62	0.58	0.37	0.49	0.6	0.53	1.88	1.06	0.73
log. decrement	δ_s	[-]	0.03	0.014	0.03	0.025	0.02	0.02	0.03	0.02	0.04
Scruton number	Sc	[-]	5.88	3.03	4.08	4.77	6	10.4	6.1	6.5	8.87
Strouhal number	St	[-]	0.2	0.2	0.2	0.2	0.2	0.2	0.2	0.2	0.14
critical velocity	u.crit	[m/s]	6.8	8.1	4.4	4.4	4.8	10.5	11.8	4.3	8.4
Reynolds number	Re	[-]	1.0E+06	1.5E+06	7.1E+05	5.3E+05	5.1E+05	2.8E+06	9.8E+05	2.4E+05	9.0E+05
mass ratio	$m/\rho d^2$	[-]	108	108	68	95	150	260	102	163	111
shape factor	C	[-]	0.0100	0.0100	0.0075	0.0054	0.0052	0.0100	0.0098	0.0120	0.0092
amplitude factor	a_L	[-]	0.4	0.4	0.4	0.4	0.4	0.4	0.4	0.4	0.4
turbulence intensity	I_v	[%]	0	0	0	0	0	0	15	0	0
aerodynamic damp.	K_a	[-]	1.00	1.00	0.75	0.54	0.52	1.00	0.54	1.20	0.92
relative amplitude	σ_y/d	[-]	0.278	0.349	0.302	0.219	0.111	0.166	0.131	0.302	0.197
peak-factor	k_p	[-]	1.46	1.41	1.41	1.93	2.38	2.20	2.46	1.41	2.10
relative max. amplitude	y_{max}/d	[-]	0.41	0.49	0.43	0.42	0.26	0.37	0.32	0.43	0.41
measured / observed	y_{max}/d	[-]	0.23	0.36	0.42	0.28	0.25	0.17	0.20	0.37	0.31
measured / observed	y_{max}	[mm]	500 (O)	1000 (O)	1000 (O)	500 (O)	400 (M)	690 (M)	250 (O)	300 (O)	500 (O)

Table 3. Chimneys from Germany.

Identification — location:			Aachen Germany	Köln Germany	Pirna Germany	Pirna Germany	Reckling. Germany
Reference:							
Measured / estimated refer to damping:			Meas.	Meas.	Meas. No damp.	Meas. With damp.	Meas.
height	h	[m]	28	35	60	60	38
diameter	d	[m]	0.914	0.813	2	2	1.016
slenderness ratio	h/d	[-]	31	43	30	30	37
natural frequency	ne	[Hz]	1.72	0.612	0.802	0.77	0.68
log. decrement	δ_s	[-]	0.015	0.015	0.015	0.125	0.03
Scruton number	Sc	[-]	2.56	7.33	1.90	17.23	10.71
Strouhal number	St	[-]	0.2	0.2	0.2	0.2	0.2
critical velocity	u.crit	[m/s]	7.9	2.5	8.0	7.7	3.5
Reynolds number	Re	[-]	4.8E+05	1.3E+05	1.1E+06	1.0E+06	2.3E+05
mass ratio	m/ ρd^2	[-]	85	244	63	69	179
shape factor	C	[-]	0.0054	0.0172	0.0100	0.0100	0.0121
amplitude factor	aL	[-]	0.4	0.4	0.4	0.4	0.4
turbulence intensity	Iv	[%]	0	0	0	0	0
aerodynamic damp.	Ka	[-]	0.54	1.72	1.00	1.00	1.21
relative amplitude	σ_y/d	[-]	0.316	0.325	0.369	0.009	0.217
peak-factor	kp	[-]	1.41	1.41	1.41	3.05	1.97
maximum amplitude	y_{max}/d	[-]	0.45	0.46	0.52	0.03	0.43
measured / observed	y_{max}/d	[-]	0.38	0.48	0.25	0.03	0.07
measured / observed	y_{max}	[mm]	347 (M)	388 (M)	500 (M)	49 (M)	74 (M)

Table 4A. Chimneys from Pritchard (1984) not located in a group.

Identification — location:			Mitzushim. Japan	Chiba Japan	Wakayam. Japan	Sakai * Japan	Alderman- ston. UK	Germany	Germany	France	Canada	Stack "A"	Stack "B"***
Reference:			Nakagawa 1963	Nakagawa 1963	Nakagawa 1963	Nakagawa 1963	Scruton 1955	Ruschew. 1975	Ruschew. 1975	Exxon	Exxon	Johns et al 1972	Johns et al 1972
Measured / estimated refer to damping:			Meas.	Meas.	Meas.	Meas.	Est.	Meas.	Meas.	Est.	Est.	Meas.	Meas.
height	h	[m]	90	91.5	83	77	46	145	74	72	36	17	18.6
diameter	d	[m]	5.1	5.3	4.1	3.9	1.22	6	3	3.05	0.4	0.6	0.7
slenderness ratio	h/d	[-]	18	17	20	20	38	24	25	24	90	28	27
natural frequency	ne	[Hz]	0.8	0.8	1.2	0.7	0.9	0.5	0.7	0.8	0.4	2	1.8
log. decrement	δ_s	[-]	0.031	0.025	0.038	0.031	0.013	0.031	0.013	0.013	0.019	0.025	0.145
Scruton number	Sc	[-]	4	2.9	4.9	4.5	2.6	2.7	1.3	1.4	6.6	10.6	50
Strouhal number	St	[-]	0.2	0.2	0.2	0.2	0.2	0.2	0.2	0.2	0.2	0.2	0.2
critical velocity	u.crit	[m/s]	20.4	21.2	24.6	13.7	5.5	15.0	10.5	12.2	0.8	6.0	6.3
Reynolds number	Re	[-]	6.9E+06	7.5E+06	6.7E+06	3.5E+06	4.5E+05	6.0E+06	2.1E+06	2.5E+06	2.1E+04	2.4E+05	2.9E+05
mass ratio	m/ ρd^2	[-]	64	58	65	72	103	43	52	56	175	211	175
shape factor	C	[-]	0.0100	0.0100	0.0100	0.0100	0.0061	0.0100	0.0100	0.0100	0.0200	0.0118	0.0099
amplitude factor	aL	[-]	0.4	0.4	0.4	0.4	0.4	0.4	0.4	0.4	0.4	0.4	0.4
turbulence intensity	Iv	[%]	15	15	15	15	0	15	15	15	0	0	0
aerodynamic damp.	Ka	[-]	0.55	0.55	0.55	0.55	0.61	0.55	0.55	0.55	2.00	1.18	0.99
relative amplitude	σ_y/d	[-]	0.260	0.305	0.216	0.237	0.325	0.313	0.361	0.357	0.344	0.215	0.005
peak-factor	kp	[-]	1.56	1.45	1.73	1.64	1.43	1.44	1.42	1.42	1.42	1.74	3.5
relative max. amplitude	y_{max} / d	[-]	0.40	0.44	0.37	0.39	0.46	0.45	0.51	0.51	0.49	0.37	0.02
measured / observed	y_{max} / d	[-]	0.06	0.06	0.06	0.02	0.25	0.2	0.46	0.33	0.5	0.17	0.07

Notes * This chimney is fitted with a type of helical spoiler

** This chimney is supported upon resilient damping pads

Table 4B. Chimneys from Pritchard (1984) not located in a group.

Identification — location:			Greece	England	Netherla.	Netherla.	Netherla.	USA No. 31	UK	Netherla. NE	Netherla. Nho	Netherla. Nlv
Reference:			Exxon	Exxon	Van Koten 1979	Van Koten 1979	Van Koten 1979	Zorilla 1972	Pritchard Pers. C.	Pritchard Pers. C.	Pritchard Pers. C.	Pritchard Pers. C.
Measured / estimated refer to damping:			Est.	Est.	Est.	Est.	Est.	Est.	Est.	Est.	Est.	Est.
height	h	[m]	43.5	46	60	60	75	76	55	40	40	65
diameter	d	[m]	1.68	1.8	1.58	1	0.96	2.9	2.14	1	1.6	0.9
slenderness ratio	h/d	[-]	26	26	38	60	78	26	26	40	25	72
natural frequency	ne	[Hz]	0.5	0.9	0.5	0.6	0.8	0.7	1.1	0.7	1.3	0.3
log. decrement	δ_s	[-]	0.013	0.019	0.013	0.013	0.013	0.031	0.013	0.013	0.013	0.013
Scruton number	Sc	[-]	2.8	4.20	1.9	2.9	3.10	7.6	1.4	2.4	1.8	4.2
Strouhal number	St	[-]	0.2	0.2	0.2	0.2	0.2	0.2	0.2	0.2	0.2	0.2
critical velocity	u.crit	[m/s]	4.2	8.1	4.0	3.0	3.8	10.2	11.8	3.5	10.4	1.4
Reynolds number	Re	[-]	4.7E+05	9.7E+05	4.2E+05	2.0E+05	2.5E+05	2.0E+06	1.7E+06	2.3E+05	1.1E+06	8.1E+04
mass ratio	m/ ρd^2	[-]	111	111	76	115	123	121	56	95	72	167
shape factor	C	[-]	0.0056	0.0098	0.0067	0.0135	0.0116	0.0100	0.0100	0.0121	0.0100	0.0200
amplitude factor	aL	[-]	0.4	0.4	0.4	0.4	0.4	0.4	0.4	0.4	0.4	0.4
turbulence intensity	lv	[%]	0	0	0	0	0	0	15	0	15	0
aerodynamic damp.	Ka	[-]	0.56	0.98	0.67	1.35	1.16	1.00	0.55	1.21	0.55	2.00
relative amplitude	σ_y/d	[-]	0.310	0.325	0.352	0.364	0.355	0.252	0.357	0.367	0.344	0.365
peak-factor	kp	[-]	1.45	1.43	1.42	1.42	1.42	1.58	1.42	1.42	1.42	1.42
relative max. amplitude	y_{max} / d	[-]	0.45	0.46	0.50	0.52	0.50	0.40	0.51	0.52	0.49	0.52
measured / observed	y_{max} / d	[-]	0.21	0.17	0.25	0.4	0.4	0.17	0.18	0.28	0.3	0.45